Raman spectroscopy of newberyite, hannayite and struvite.

Ray L. Frost[•] [a], Matt L. Weier [a], Wayde N. Martens, [a] Dermot A. Henry [b], and Stuart J. Mills [b,c]

[a] Inorganic Materials Research Program, School of Physical and Chemical Sciences, Queensland University of Technology, GPO Box 2434, Brisbane Queensland 4001, Australia.

[b] Geosciences, Museum Victoria, PO Box 666E, Melbourne, Victoria 3001, Australia.

[c] CSIRO Minerals, Box 312, Clayton South, Victoria 3169, Australia.

This is the authors' version of a paper that was later published as:

Frost, Ray, Weier, Matt , Martens, Wayde, Henry, Dermot & Mills, Stuart (2005) Raman spectroscopy of newberyite, hannayite and struvite. *Spectrochimica Acta* 62(1):pp. 181-188.

Abstract

The phosphate minerals hannayite, newberyite and struvite have been studied by Raman spectroscopy using a thermal stage. Hannayite and newberyite are characterised by an intense band at around 980 cm^{-1} assigned to the ν_1 symmetric stretching vibration of the HPO_4 units. In contrast the symmetric stretching mode is observed at 942 cm^{-1} for struvite. The Raman spectra are characterised by multiple ν_3 antisymmetric stretching bands and ν_2 and ν_4 bending modes indicating strong distortion of the HPO_4 and PO_4 units. Hannayite and newberyite are defined by bands at 3382 and 3350 cm^{-1} attributed to $HOPO_3$ vibrations and hannayite and struvite by bands at 2990, 2973 and 2874 assigned to NH_4^+ bands. Raman spectroscopy has proven most useful for the analysis of these 'cave' minerals where complex paragenetic relationships exist between the minerals.

Keywords: hannayite, newberryite, struvite, phosphate, Raman spectroscopy

Introduction

Interest in struvite formation also comes from the formation in urinary tracts and kidneys [1-6]. Indeed the discovery of newberyite have been found in very old and large calculi [7]. Newberyite is found as a decomposition product of ivory. More often than not the presence of struvite has been determined by infrared spectroscopy [8-16]. On occasions Raman spectroscopy has also been used to study the presence of struvite in urine [9, 17, 18]. The mineral struvite has the formula ($NH_4MgPO_4.6H_2O$) and is orthorhombic [19]. The mineral is related to dittmarite ($NH_4MgPO_4.H_2O$),

[•] Author to whom correspondence should be addressed (r.frost@qut.edu.au)

niahite ($NH_4(Mn,Mg)PO_4.6H_2O$), hannayite ($(NH_4)_2Mg(HPO_4)_4.6H_2O$), schertelite ($(NH_4)_2MgH_2(PO_4)_4.4H_2O$), stercorite ($Na(NH_4)_2HPO_4.4H_2O$), swaknoite ($Ca(NH_4)_2(HPO_4)_2.H_2O$), and mundrabillaite ($(NH_4)_2CaHPO4.H_2O$). Many of these minerals are found in caves and are the result of formation from guano [20-24].

Often infrared spectroscopy is used to study these minerals in the urinary tracts and calculi [9, 25-28]. The amount of published data on the Raman spectra of mineral phosphates is limited [29-33]. The Raman spectra of the hydrated hydroxy phosphate minerals have not been reported. In aqueous systems, Raman spectra of phosphate oxyanions show a symmetric stretching mode (ν_1) at 938 cm^{-1}, the antisymmetric stretching mode (ν_3) at 1017 cm^{-1}, the symmetric bending mode (ν_2) at 420 cm^{-1} and the ν_4 mode at 567 cm^{-1} [31, 32, 34]. S.D. Ross in Farmer (1974) (page 404) listed some well-known minerals containing phosphate which were either hydrated or hydroxylated or both [35]. The value for the ν_1 symmetric stretching vibration of PO_4 units as determined by infrared spectroscopy was given as 930 cm^{-1} (augelite), 940 cm^{-1} (wavellite), 970 cm^{-1} (rockbridgeite), 995 cm^{-1} (dufrenite) and 965 cm^{-1} (beraunite). The position of the symmetric stretching vibration is mineral dependent and a function of the cation and crystal structure. The fact that the symmetric stretching mode is observed in the infrared spectrum affirms a reduction in symmetry of the PO_4 units. Some studies have been undertaken on $MgHPO_4.3H_2O$ [36, 37]. It is not known whether a mineral was studied or whether a synthetic chemical was used. Infrared bands were found at 1162, 1057 and 1017 cm^{-1} and were assigned to the ν_3 antisymmetric stretching modes. Some more recent studies of newberyite have been undertaken [26, 38].

The value for the ν_2 symmetric bending vibration of PO_4 units as determined by infrared spectroscopy was given as 438 cm^{-1} (augelite), 452 cm^{-1} (wavellite), 440 and 415 cm^{-1} (rockbridgeite), 455, 435 and 415 cm^{-1} (dufrenite) and 470 and 450 cm^{-1} (beraunite). The observation of multiple bending modes provides an indication of symmetry reduction of the PO_4 units. This symmetry reduction is also observed through the ν_3 antisymmetric stretching vibrations. Augelite shows infrared bands at 1205, 1155, 1079 and 1015 cm^{-1}; wavellite at 1145, 1102, 1062 and 1025 cm^{-1}; rockbridgeite at 1145, 1060 and 1030 cm^{-1}; dufrenite at 1135, 1070 and 1032 cm^{-1}; beraunite at 1150, 1100, 1076 and 1035 cm^{-1}. Some Raman spectra have been published [26, 27]. The studies of the synthetic newberyite showed bands at 398 cm^{-1} assigned to the ν_2 bending mode and at 554 and 509 cm^{-1} corresponding to the ν_4 bending modes [37, 39].

The detailed comparative Raman spectra of the minerals newberyite, hannayite and struvite have not been published. Often the hydroxyl and NH_4^+ stretching vibrations are not given and only the PO_4 or HPO_4 vibrational modes are given. This paper reports the vibrational spectra of these minerals and related the spectra to the known crystal structures.

Experimental

Minerals

Two newberyite samples were obtsianed from Museum Victoria, samples M25186 and M 14824. These minerals originated from Lava Cave, 5 km S of Skipton (37 44 30 S, 143 21 30 E) , Skipton, Victoria, Australia. The mineral hannayite (sample M 13417**)** was obtained from the same place. The minerals were analysed for phase purity by X-ray diffraction and the compositions were checked by EDX analyses.

Raman microprobe spectroscopy

Samples of the minerals were placed and orientated on the stage of an Olympus BHSM microscope, equipped with 10x and 50x objective lenses, as part of a Renishaw 1000 Raman microscope system. This system also includes a monochromator, filter system and a Charge Coupled Device (CCD). Raman spectra were excited by a HeNe laser (633 nm) at a resolution of 2 cm^{-1} in the range between 100 and 4000 cm^{-1}. Repeated acquisition using the highest magnification was undertaken to improve the signal-to-noise ratio. Spectra were calibrated using the 520.5 cm^{-1} line of a silicon wafer. In order to ensure that the correct spectra were obtained, the incident excitation radiation was scrambled. Previous studies provide an in depth account of the experimental technique [31, 40-44]. Spectral manipulation such as baseline adjustment, smoothing and normalisation was performed using the GRAMS® software package (Galactic Industries Corporation, Salem, NH, USA).

Infrared absorption spectroscopy

Infrared spectra were obtained using a Nicolet Nexus 870 FTIR spectrometer with a smart endurance single bounce diamond ATR cell. Spectra over the 4000–525 cm^{-1} range were obtained by the co-addition of 64 scans with a resolution of 4 cm^{-1} and a mirror velocity of 0.6329 cm/s.

Results and discussion

The Raman spectra of hannayite and newberyite are shown in a set of figures according to the wavenumber region. Figure 1 displays the hydroxy and NH_4 stretching region of hannayite; Figure 2 the OH and NH_4 stretching region of newberyite and struvite; Figure 3 the 800 to 2000 cm^{-1} region of hannayite; Figure 4 the 1300 to 2000 cm^{-1} region of newberyite and struvite; Figure 5 shows the low wavenumber region of hannayite and Figure 6 the low wavenumber region of struvite and hannayite. The analyses of the Raman spectral data are collected in Table 1 (hannayite) and in Table 2 (struvite and newberyite).

The Raman spectrum of hannayite at 298 K shows a series of bands at 3496, 3460, 3384, 3314, 3219, 3185, 3125, 3090, 2983 and 2872 cm^{-1}. These bands are attributed to a mixture of the hydroxyl and NH_4 stretching vibrations. Further hannayite is a mineral which contains HPO_4 units and hence there will be $HOPO_3$ vibrations. The Raman spectrum of hannayite is more well defined at 77 K. Raman bands are observed at 3382, 3350, 3217, 3179, 3132, 3120, 2990, 2973 and 2874 cm^{-1}.

In comparison the infrared spectrum shows a spectral profile made up of a series of overlapping bands. According to Catti and Franchini-Angela the structure of hannayite consists of layers of P and Mg coordination polyhedra sharing vertices [45]. Layers are linked by H bonds of H_2O and NH_4^+ ions, and are formed by 2 crossing systems of [001] double chains and [111] single chains of polyhedra. A distorted coordination is shown by the W(1) water molecule [45]. The NH_4^+ ion has a coordination no. of six, with 4 ordered H bonds tetrahedrally arranged and 2 electrostatic bonds. The 77 K Raman spectrum may be divided into three sets of bands. These are (a) the bands at 3382 and 3350 cm^{-1} attributed to $HOPO_3$ vibrations, (b) bands in the 3120 to 3217 cm^{-1} region ascribed to water stretching bands, and (c) the bands at 2990, 2973 and 2874 assigned to NH_4^+ bands. The mineral newberyite does not have any NH_4^+ units. No bands are observed in the Raman spectra of newberyite between 2800 and 3150 cm^{-1}. This observation confirms the bands for hannayite in this region to NH_4^+ vibrations.

The Raman spectrum of newberyite shows a series of bands at 3514, 3479, 3456, 3381, 3265 and 3180 cm^{-1} at 298 K and 3501, 3468, 3364, 3244 and 3277 cm^{-1} at 77 K. The crystal structure of newberyite has been solved [46]. The structure is orthorhombic with 8 formula units per unit cell. The structure is strongly distorted. In the 77 K spectrum the two bands at 3501 and 3468 cm^{-1} are assigned to the –POH vibrations in line with the assignment of the bands for hannayite. The bands at 3364, 3244 and 3227 cm^{-1} are assigned to the water stretching vibrations. There are no bands attributable to NH_4 units in newberyite.

The Raman and IR spectra of hannayite are shown in Figure 3. The Raman spectra are dominated by a single intense band at 974 cm^{-1} in the 298 K spectrum and at 272 in the 77 K spectrum. The band is sharp with bandwidths of 11.2 and 6.2 cm^{-1} respectively. This band is attributed to the HPO_4 symmetric stretching vibration. In the infrared spectrum two bands are observed at 1009 and 984 cm^{-1} and are attributed to the infrared activated PO_4 symmetric stretching vibration. Normally such a vibration should not be observed but because of the distortion of the PO_4 units in the hannayite structure the bands become infrared-active. For newberyite, at 298 K an intense band attributed to the PO_4 symmetric stretching vibration is observed at 984 cm^{-1} with band with of 12.1 cm^{-1}. The band is found at 984 cm^{-1} with a bandwidth of 7.1 cm^{-1} at 77 K. In the infrared spectrum two bands are observed at 994 and 1016 cm^{-1}. For struvite the PO_4 symmetric stretching band is observed at 942 cm^{-1}. The difference in the band positions for the struvite as compared with the hannayite and newberyite is that struvite contains PO_4 units where as the other two minerals contain HPO_4 units.

In the Raman spectrum of hannayite three bands are observed at 1172, 1070 and 1011 cm^{-1} at 298 K and at 1179, 1070 and 1012 cm^{-1}. These bands are attributed to the HPO_4 antisymmetric stretching modes. The Raman data is in agreement with published infrared data for synthetic $MgHPO_4.3H_2O$ where IR bands were found at 1162, 1057 and 1017 cm^{-1}. Our ATR spectrum of hannayite is a complex set of overlapping bands. Bands are observed at 1179, 1070and 1009 cm^{-1} together with other low intensity bands. In the Raman spectrum of newberyite only a low intensity band at 1154 cm^{-1} is observed (1162 cm^{-1} at 77 K). In the ATR spectrum three bands are observed at 1161, 1071, and 1055 cm^{-1}. These bands are attributed to the HPO_4

antisymmetric stretching modes. For struvite only low intensity Raman bands at 1076 and 1013 cm^{-1} are observed.

The Raman spectra of hannayite in the low wavenumber region are shown in Figure 5. A band is observed in the 298 K spectrum at 556 cm^{-1} of half width of 36.1 cm^{-1} which splits into two bands at 574 and 555 cm^{-1} at 77 K of half width 11.1 and 8.8 cm^{-1}. These bands are attributed to the PO_4 ν_4 bending mode. Published spectra of newberyite gave the two bands at 554 and 509 cm^{-1} as the ν_4 bending modes [37, 39]. A Raman band was observed at 522 cm^{-1} which shifted to 518 cm-1 at 77 K which may also be ascribed to a the ν_4 bending mode. In the infrared spectrum a broad band is observed at 531cm^{-1} which may be the corresponding infrared band. In the Raman spectrum of newberyite, a broad band is observed at 555 cm^{-1} which appears to split into four bands at 557, 537, 522 and 504 cm^{-1} at 77 K. The observation of multiple ν_4 bending modes is a strong indication of the reduction of symmetry of the HPO_4 ion. For struvite the ν_4 bending mode is observed at 564 cm^{-1}. Two bands are observed in the ATR spectrum at 567 and 552 cm^{-1} which may be assigned to this vibration.

In the Raman spectrum of hannayite Raman bands are observed at 436, 415, and 375 cm^{-1} which may be assigned to the PO_4 ν_2 bending modes. These bands become more clearly resolved in the 77 K spectrum where bands are observed at 424, 403 and 385 cm^{-1}. bands in these positions are not observed in the ATR spectrum as the bands are below the limit of the ATR method. The Raman spectrum of newberyite shows an intense band at 399.8 cm^{-1}. At 77 K the band splits into three bands at 409, 400 and 384 cm^{-1}. The mineral struvite's Raman spectrum displays two bands at 463 and 428 cm^{-1} which can be assigned ti this vibrational mode.

In the Raman spectrum of hannayite at 77 K a series of bands are found at 277, 254, 237, 221 and 197 cm^{-1}. The first band is of significant intensity and is attributed to the MgO stretching vibration. The band at 197 cm^{-1} may be due to the OMgO bending mode. For newberyite intense bands in the 298 K spectrum are observed at 283 and 219 cm^{-1}. The Raman spectrum of struvite also shows an intense band at 300 cm^{-1} which is attributed to the MgO stretching vibration.

Conclusions

The minerals hannayite, newberyite and struvite may be termed 'cave' minerals. These mineral formed through deposits on walls of bat excrement have been analysed by Raman spectroscopy in combination with a thermal stage. The minerals hannayite and newberyite contain hydrogen phosphate units (HPO_4) where as struvite is based upon phosphate units (PO_4). The HPO_4 and PO_4 units are characterised by intense sharp bands at 980 cm^{-1} and 942 cm^{-1}. Characteristic POH stretching bands are observed at 3382 and 3350 cm^{-1}. Such bands are absent in the Raman spectrum of struvite. Hannayite and struvite contain NH_4^+ units which are observed by NH stretching vibrations at 2990, 2973 and 2874. The use of a portable Raman spectrometer would enable the identification of such 'cave' minerals. In particular where close paragenetic relationships exist between these minerals Raman spectroscopy enables the identification and study of such minerals.

Acknowledgements

The financial and infrastructure support of the Queensland University of Technology Inorganic Materials Research Program of the School of Physical and Chemical Sciences is gratefully acknowledged. The Australian Research Council (ARC) is thanked for funding. Museum Victoria is thanked for the loan of the minerals. SJM wishes to thank the support of CSIRO Minerals.

References

[1]. H. J. Schneider and M. Anke, Urologia 24 (1969) 300.
[2]. H. J. Schneider, L. Klotz and G. Horn, Urologia 62 (1969) 351.
[3]. H. J. Schneider, Urologia 62 (1969) 123.
[4]. H. J. Schneider and G. Horn, Urologia 61 (1968) 753.
[5]. H. J. Schneider and M. Anke, Urologia 61 (1968) 361.
[6]. H. J. Schneider and M. Anke, Urologia 61 (1968) 361.
[7]. K. Lonsdale and D. J. Sutor, Science 154 (1966) 1353.
[8]. M. Daudon, C. Marfisi, B. Lacour and C. Bader, Clin. Chem. 37 (1991) 83.
[9]. M. Daudon, M. F. Protat, R. J. Reveillaud and H. Jaeschke-Boyer, Kidney International 23 (1983) 842.
[10]. E. Escolar and J. Bellanato, Biospec. 5 (1999) 237.
[11]. M. H. Gault, M. Ahmed, J. Kalra, I. Senciall, J. Morgan, W. Cohen and D. Churchill, Urolithiasis: Clincial Basic Res., [Proc. Int. Symp.], 4th (1981) 993.
[12]. A. Hesse, M. Gergeleit, P. Schueller and K. Moeller, J. Clin. Chem. Clin. Biochem. 27 (1989) 639.
[13]. A. Khaliq, J. Ahmed and N. Khalid, British J. Urol. 56 (1984) 135.
[14]. W. E. Klee, Fortschritte der Urologie und Nephrologie 9 (1977) 234.
[15]. Y. G. Kozlovsky, M. M. Shokarev and F. I. Vershinina, Laboratornoe Delo (1977) 659.
[16]. C. Paluszkiewicz, M. Galka, W. Kwiatek, A. Parczewski and S. Walas, Biospec. 3 (1997) 403.
[17]. K. Sudlow and A. Woolf, Clinica Chimica Acta 203 (1991) 387.
[18]. K. Angoni, J. Popp and W. Kiefer, Spec. Letts. 31 (1998) 1771.
[19]. J. A. Bland and S. J. Basinski, Nature 183 (1959) 1385.
[20]. P. J. Bridge, Min. Mag. 39 (1973) 467.
[21]. P. J. Bridge, Min. Mag. 41 (1977) 33.
[22]. P. J. Bridge and R. M. Clark, Min. Mag. 47 (1983) 80.
[23]. P. J. Bridge and B. W. Robinson, Min. Mag. 47 (1983) 79.
[24]. R. J. Bowell, A. Warren and I. Redmond, Geol. Soc. Special Publication 113 (1996) 63.
[25]. M. Modlin and P. J. Davies, South African Medical Journal 59 (1981) 337.
[26]. B. Soptrajanov, G. Jovanovski, I. Kuzmanovski and V. Stefov, Spec. Letts 31 (1998) 1191.
[27]. B. Soptrajanov, I. Kuzmanovski, V. Stefov and G. Jovanovski, Spec. Letts 32 (1999) 703.
[28]. M. Volmer, J. C. M. De Vries and H. M. J. Goldschmidt, Clin. Chem. 47 (2001) 1287.
[29]. R. L. Frost, L. Duong and W. Martens, Neues Jahrbuch fuer Mineralogie, Monatshefte (2003) 223.
[30]. R. L. Frost, W. Martens, P. A. Williams and J. T. Kloprogge, J.Ram. Spec. 34 (2003) 751.
[31]. R. L. Frost, W. Martens, P. A. Williams and J. T. Kloprogge, Min. Mag. 66 (2002) 1063.
[32]. R. L. Frost, P. A. Williams, W. Martens, J. T. Kloprogge and P. Leverett, J. Ram. Spec. 33 (2002) 260.

[33]. R. L. Frost, P. A. Williams, W. Martens and J. T. Kloprogge, J. Ram. Spec.33 (2002) 752.
[34]. R. L. Frost, W. N. Martens, T. Kloprogge and P. A. Williams, Neues Jahrbuch fuer Mineralogie, Monatshefte (2002) 481.
[35]. V. C. Farmer, *Mineralogical Society Monograph 4: The Infrared Spectra of Minerals*, 1974.
[36]. F. A. Miller, G. L. Carlson, F. F. Bentley and W. H. Jones, Spectrochim. Acta 16 (1960) 135.
[37]. F. A. Miller and C. H. Wilkins, Anal. Chem. 24 (1952) 1253.
[38]. I. L. Shashkova, N. V. Kitikova, A. I. Rat'ko and A. G. D'yachenko, Inorg. Mats. (Translation of Neorganicheskie Materialy) 36 (2000) 826.
[39]. J. R. Lehr, E. H. Brown, A. W. Frazier, J. P. Smith and R. D. Thrasher, Tennessee Valley Authority, Chemical Engineering Bulletin No. 6 (1967) 166 pp.
[40]. R. L. Frost, M. Crane, P. A. Williams and J. T. Kloprogge, J. Ram. Spec. 34 (2003) 214.
[41]. R. L. Frost, P. A. Williams and W. Martens, Min. Mag. 67 (2003) 103.
[42]. W. Martens, R. L. Frost and J. T. Kloprogge, J. Ram. Spec.34 (2003) 90.
[43]. W. Martens, R. L. Frost, J. T. Kloprogge and P. A. Williams, J. Ram. Spec. 34 (2003) 145.
[44]. R. L. Frost, W. Martens, J. T. Kloprogge and P. A. Williams, J. Ram. Spec. 33 (2002) 801.
[45]. M. Catti and M. Franchini-Angela, Acta Cryst. B32 (1976) 2842.
[46]. D. J. Sutor, Acta Cryst. 23 (1967) 418.

Table 1 Results of the vibrational spectroscopy of hannayite

ATR			298K Raman			77K Raman		
Center	FWHM	Area	**Center**	FWHM	Area	**Center**	FWHM	Area
3490	29.7	0.005	**3496**	26.6	0.006			
3483	103.2	0.046						
			3460	118.7	0.030			
3424	36.8	0.002						
3373	89.1	0.081	**3384**	70.7	0.024	**3382**	39.8	0.020
						3350	19.4	0.058
			3314	79.6	0.015			
3288	95.7	0.032						
			3219	109.2	0.049	**3217**	52.9	0.066
3199	137.9	0.135	**3185**	44.5	0.017	**3179**	37.1	0.103
			3125	40.1	0.021	**3132**	14.4	0.018
3111	39.8	0.006				**3120**	35.5	0.093
3066	171.0	0.143	**3090**	105.0	0.029			
			2983	119.0	0.037	**2990**	43.1	0.059
2966	100.4	0.044				**2973**	14.1	0.035
2875	19.5	0.001	**2872**	61.8	0.015	**2874**	18.7	0.065
2865	59.7	0.011						
2827	193.4	0.102						
2680	108.6	0.011						
			2649	122.0	0.012			
2456	70.6	0.007	**2466**	209.5	0.045			
2392	49.3	0.005						
2306	222.6	0.029						
			2228	100.0	0.005			
			1947	170.0	0.044			
1890	36.1	0.001						
1812	95.7	0.005						
			1756	302.4	0.149			
1698	41.3	0.004	**1708**	21.7	0.003	**1713**	9.0	0.014
1652	42.2	0.007	**1661**	85.5	0.009			
1635	181.0	0.026						
1486	81.1	0.002						
1459	11.7	0.002	**1457**	21.1	0.001	**1459**	25.1	0.021
1448	31.2	0.016						
1444	11.3	0.002	**1429**	136.2	0.073			
1415	40.9	0.004						
1294	31.3	0.007						
1250	32.2	0.005						
			1227	67.7	0.012			
1179	31.9	0.017	**1172**	73.3	0.022	**1179**	4.3	0.007
1158	16.6	0.002						
1142	18.6	0.010						
			1119	23.1	0.001			
1070	55.4	0.064	**1070**	12.6	0.002	**1070**	6.6	0.007
1056	21.0	0.003				**1067**	31.0	0.021
1009	23.3	0.012	**1011**	11.4	0.002	**1012**	6.2	0.021
984	28.8	0.037				**999**	8.5	0.005
			974	11.2	0.026	**972**	6.2	0.161
965	49.8	0.020	**971**	92.8	0.029			

924	33.1	0.004						
890	11.6	0.002	**882**	14.4	0.001	**887**	14.7	0.024
880	27.4	0.013						
848	49.7	0.007						
						819	21.5	0.016
			802	52.6	0.008			
765	90.1	0.018	**757**	63.6	0.014			
636	55.3	0.007				**611**	12.5	0.004
			596	73.8	0.020			
581	18.0	0.001				**574**	11.1	0.012
			556	36.1	0.008	**555**	8.8	0.018
531	77.9	0.002						
			522	8.9	0.003	**518**	16.6	0.007
			513	112.7	0.018			
			436	14.4	0.001			
			415	26.4	0.002	**424**	24.5	0.021
						403	7.3	0.010
			379	155.9	0.052	**385**	19.8	0.040
			375	15.2	0.001			
			356	27.0	0.001			
			269	9.6	0.000	**277**	9.2	0.021
			250	7.4	0.001	**254**	9.8	0.002
			247	57.1	0.018	**237**	3.9	0.006
			205	22.5	0.007	**221**	4.8	0.008
			193	16.2	0.003	**197**	11.1	0.015
						178	7.5	0.006
						157	7.3	0.002

Table 2

Struvite ATR			Struvite 298K Raman			Newberyite ATR			Newberyite 298K Raman			Newberyite 77K Raman		
Center	FWHM	Area	**Center**	FWHM	Area	**Center**	FWHM	Area	**Center**	FWHM	Area	**Center**	FWHM	Area
3583.5	61.1	0.002				**3535.9**	39.8	0.002						
						3515.1	23.3	0.004	**3514.0**	48.0	0.029	**3501.2**	13.1	0.031
						3488.7	128.1	0.080						
3471.8	142.2	0.010				**3474.3**	22.5	0.003	**3479.3**	26.6	0.080	**3468.5**	12.3	0.082
									3456.0	62.1	0.073			
						3376.7	78.8	0.041	**3381.1**	92.3	0.153	**3364.0**	27.2	0.018
						3263.8	92.5	0.089	**3265.4**	85.1	0.135			
			3239.3	95.8	0.023							**3244.5**	42.6	0.193
						3216.9	265.9	0.214				**3227.4**	20.6	0.054
3169.7	294.2	0.069							**3180.8**	80.3	0.019			
			3115.2	204.5	0.181									
			2921.4	143.3	0.083									
			2902.8	6.8	0.001									
2867.7	400.6	0.530				**2866.2**	329.9	0.119	**2879.6**	160.2	0.050	**2384.4**	54.0	0.029
2507.6	313.5	0.073												
						2474.4	43.2	0.004						
						2401.8	78.8	0.010						
			2367.6	135.1	0.041									
2331.8	163.4	0.059				**2322.3**	113.8	0.012						
1803.0	179.8	0.010												
						1697.5	44.5	0.014						
1674.8	60.0	0.005										**1669.2**	52.4	0.039
						1648.3	31.5	0.024	**1648.3**	23.3	0.015	**1649.7**	10.9	0.009
						1625.4	113.6	0.016	**1619.8**	93.8	0.030			
1591.1	145.8	0.043												
1440.4	58.9	0.006				**1495.9**	150.6	0.010						

									1271.8	29.6	0.010	**1279.4**	17.9	0.006
						1234.5	27.7	0.014	**1194.9**	20.2	0.004			
						1161.3	31.9	0.045	**1154.0**	14.3	0.018	**1161.7**	7.8	0.024
												1100.8	71.7	0.023
1065.4	40.9	0.003	**1076.5**	15.7	0.017	**1071.4**	53.2	0.031						
						1054.9	24.4	0.020						
			1013.4	15.4	0.014	**1016.0**	32.0	0.049						
980.4	72.5	0.074				**993.7**	65.9	0.033	**983.8**	12.1	0.089	**983.9**	7.1	0.197
			949.5	18.2	0.042				**967.1**	53.8	0.026			
			941.8	25.4	0.352									
						900.9	14.9	0.002				**908.1**	19.2	0.055
893.7	123.1	0.055	**889.6**	50.5	0.015	**881.5**	39.0	0.032	**892.6**	22.9	0.073			
747.7	121.8	0.019				**747.6**	59.6	0.007						
												714.2	20.2	0.005
678.5	69.0	0.005				**687.5**	27.0	0.001				**679.8**	116.9	0.041
						655.9	151.9	0.101						
						596.9	30.8	0.002						
567.1	23.0	0.003	**564.1**	15.5	0.094									
551.6	29.8	0.004				**548.2**	25.0	0.005	**554.8**	14.6	0.005	**557.2**	9.4	0.005
												537.0	14.8	0.015
						524.6	49.9	0.000				**522.5**	11.8	0.006
									498.4	20.0	0.032	**503.9**	5.1	0.009
			462.8	22.7	0.011									
			427.5	22.9	0.016									
												409.0	11.0	0.037
									399.8	12.7	0.076	**400.1**	7.4	0.023
									368.7	17.0	0.009	**384.4**	17.3	0.048
									327.0	8.6	0.001	**335.2**	8.2	0.009
												312.5	3.1	0.001
			299.6	22.2	0.060							**310.3**	5.9	0.004
									282.9	14.4	0.006	**287.9**	5.8	0.004
									265.7	19.3	0.003	**257.4**	8.9	0.007

	242.1	13.6	0.016		**244.4**	8.5	0.002	**242.0**	12.5	0.005
	228.5	11.5	0.015		**219.3**	10.9	0.011	**219.5**	9.9	0.007
	205.6	12.5	0.024		**199.4**	8.3	0.004	**198.9**	10.0	0.010
					180.0	9.7	0.006	**177.9**	10.4	0.011
					158.4	4.9	0.000	**157.9**	3.9	0.003
					138.5	5.2	0.001			

List of Figures

List of Tables

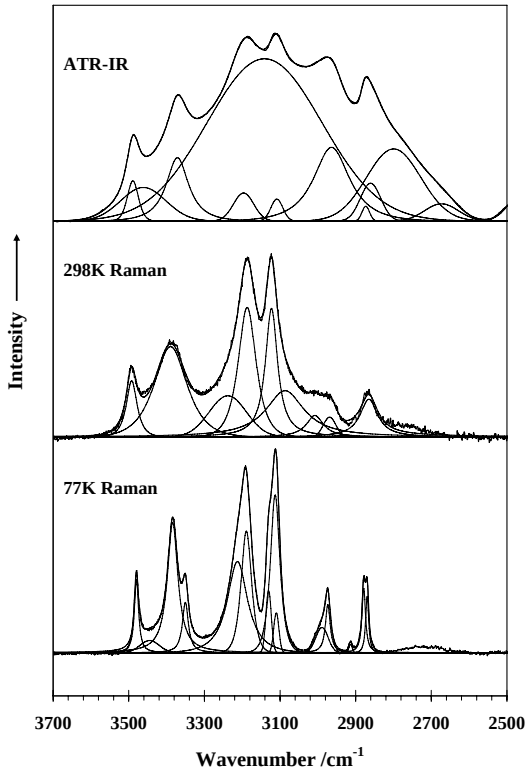

Figure 1 Hannayite

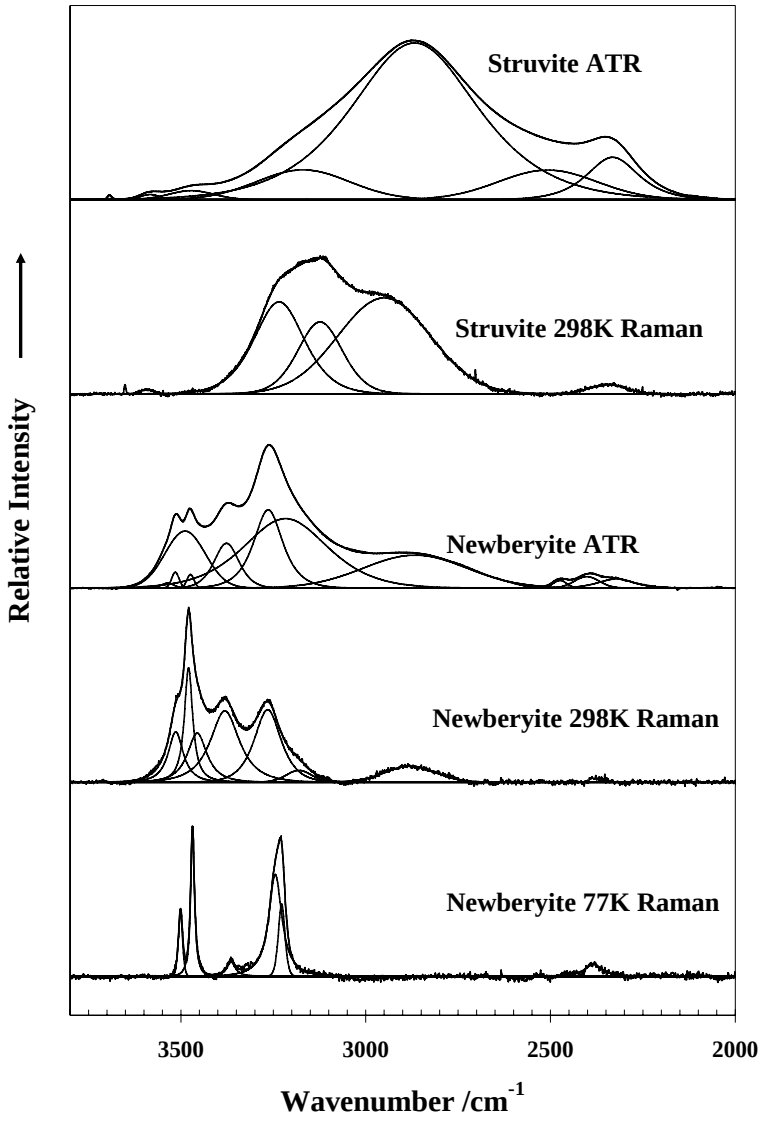
Struvite ATR
Struvite 298K Raman
Newberyite ATR
Newberyite 298K Raman
Newberyite 77K Raman
Relative Intensity
3500
3000
2500
2000
Wavenumber /cm-1

Figure 2

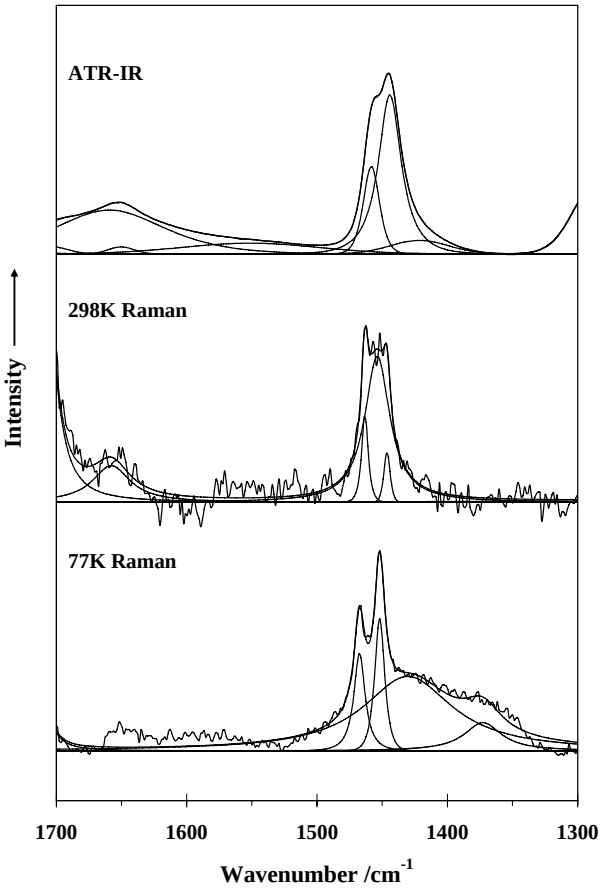
ATR-IR
298K Raman
77K Raman
Intensity
1700
1600
1500
1400
1300
Wavenumber /cm-1

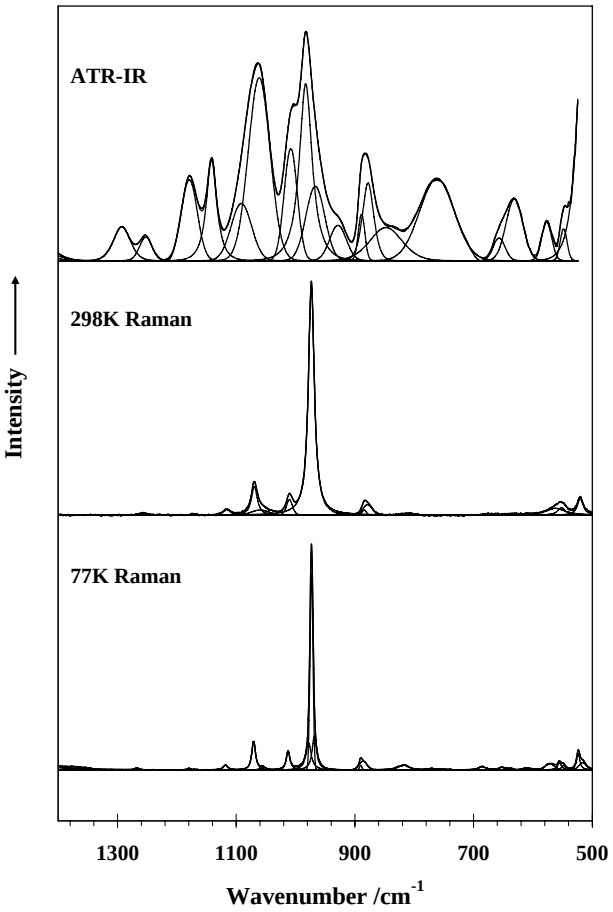

Figure 3 Hannayite

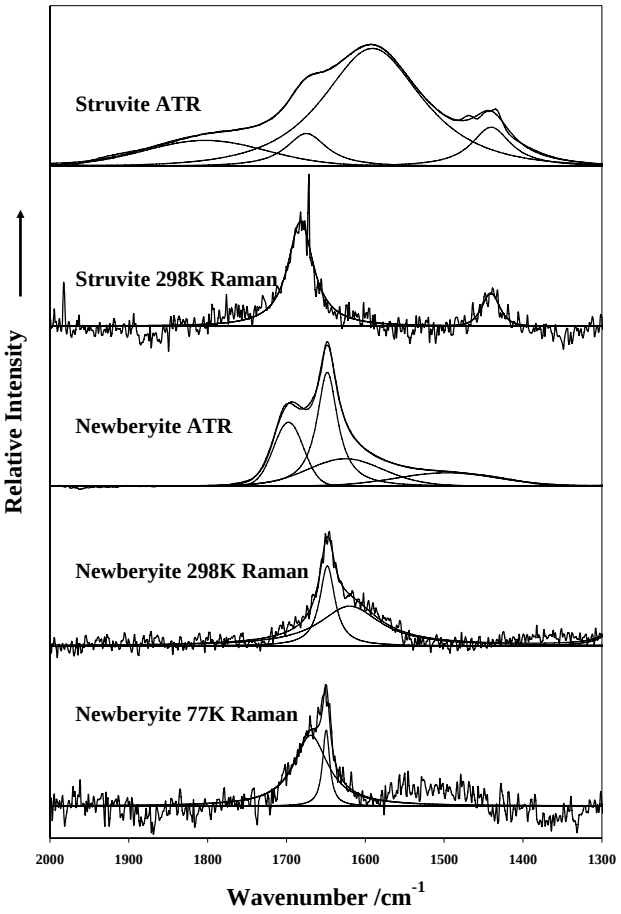

Figure 4 Newberyite

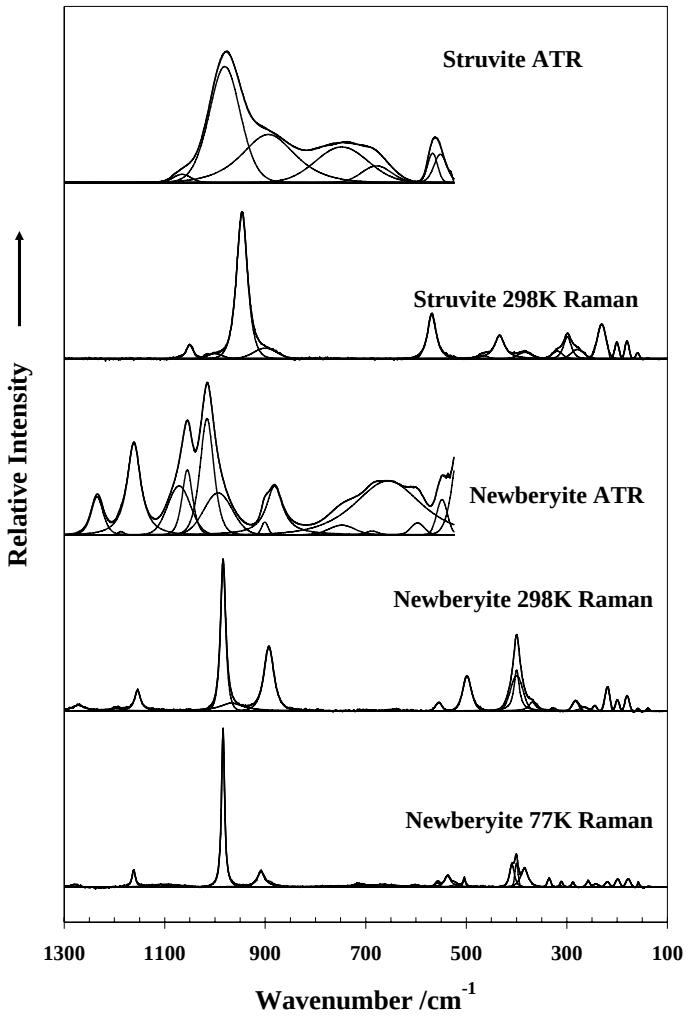
Struvite ATR
Struvite 298K Raman
Newberyite ATR
Newberyite 298K Raman
Newberyite 77K Raman
Relative Intensity
1300
1100
900
700
500
300
100
Wavenumber /cm-1

Figure 6

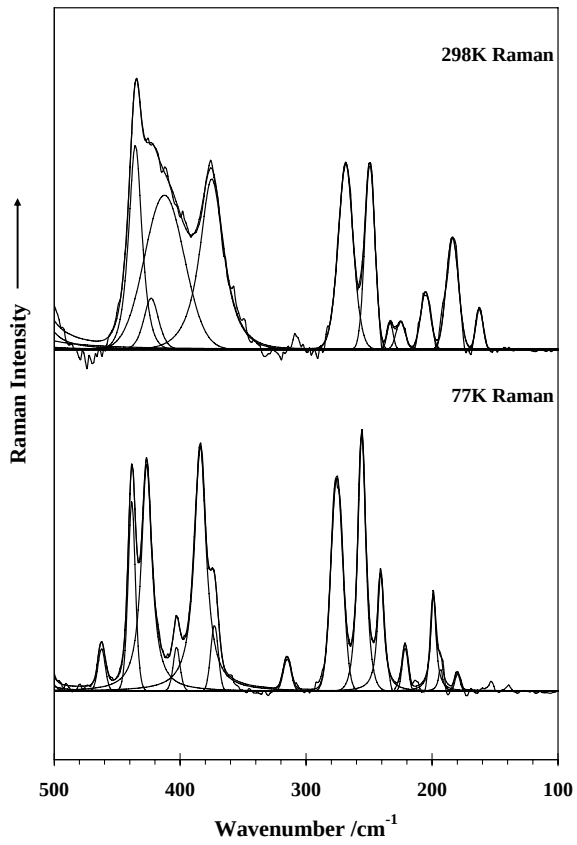

Figure 5 Hannayite